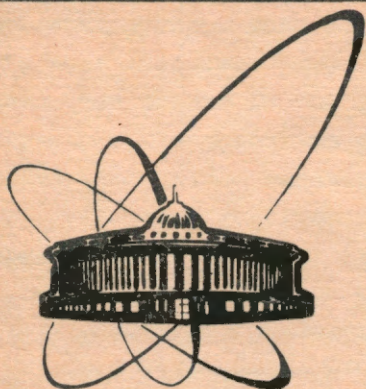


91-369



ОБЪЕДИНЕННЫЙ
ИНСТИТУТ
ЯДЕРНЫХ
ИССЛЕДОВАНИЙ
ДУБНА

E8-91-369

Yu.P.Filippov, I.A.Sergyeu

TIME-DEPENDENT RECOVERY FROM HeII FILM
BOILING: CONFINED GEOMETRY CASE

Presented at the Cryogenic Engineering Conference,
June 11-14, 1991, Huntsville, Alabama, USA.

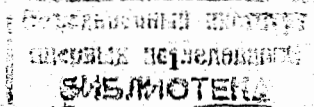
1991

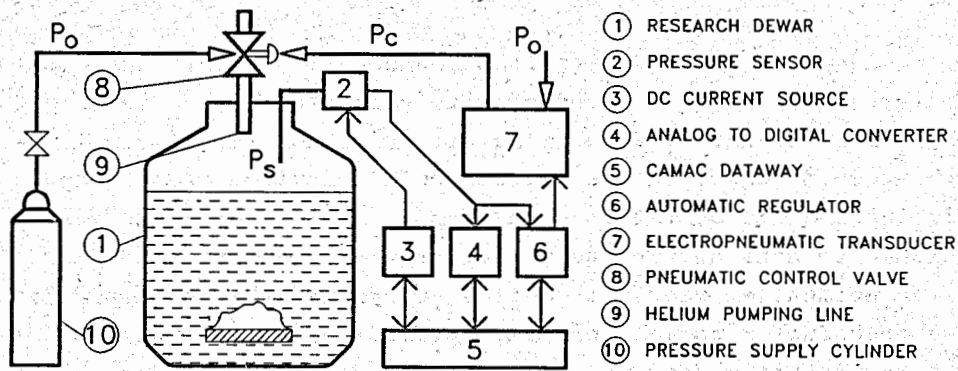
INTRODUCTION

Recovery from film boiling seems to be one of the most interesting, important and obscure problems in the transient HeII heat transfer. From time to time or regularly this phenomenon occurs in the helium-cooled devices and thereby influences the operation conditions. So, a detailed design should to consider recovery features. For example, such data are evidently required while analyzing the collapse of superconductor normal zone and optimizing the cooling down of the equipment warmed up before. A few papers are known *touching* this problem more or less closely. But only one, by Van Sciver^{1/}, presents a specific recovery study. In a one dimensional heat transfer experiment, the recovery time was observed to correlate with the energy applied to the heater during film boiling. That was explained in terms of the specimen heat capacity and the film boiling heat transfer coefficient. Our experiment configuration differs from the mentioned above and the affecting parameter variations are rather wide. The temperature decay of the heat transfer surface, $T(t)$, is measured. Evolution of the heat flux into helium, $q(t)$, is calculated from the $T(t)$ traces. A new hypothesis about the governing recovery mechanism based on the analysis of all the data $T(t)$, $q(t)$, $q(T)$ is put forward.

EXPERIMENTAL ARRANGEMENT

Pressure control. Experiment is carried out in a pool of saturated superfluid helium under conventional pumping of the vapor over the free liquid surface. Relatively high energy, up to 50 J, is applied to a heater to develop the film boiling. That conditions the pressure to rise above the saturation point in the cryostat. As a deviation from equilibrium would be unacceptable, an apparatus is employed to regulate the vapor pumping rate. The system parts and their interfunctioning are shown in Fig. 1. It should be pointed out that the microprocessor-based unit (entry 6 on





- ① RESEARCH DEWAR
- ② PRESSURE SENSOR
- ③ DC CURRENT SOURCE
- ④ ANALOG TO DIGITAL CONVERTER
- ⑤ CAMAC DATAWAY
- ⑥ AUTOMATIC REGULATOR
- ⑦ ELECTROPNEUMATIC TRANSDUCER
- ⑧ PNEUMATIC CONTROL VALVE
- ⑨ HELIUM PUMPING LINE
- ⑩ PRESSURE SUPPLY CYLINDER

Fig.1. Automatic pressure control and stabilization system. Pressures: P_s - saturated vapor, P_c - control, P_o - supply.

Fig. 1) handles a residual from a reference and a sensor readout by the PID algorithm. While test running the peak pressure drift is kept within 3%.

Heat transfer configuration. Test sample, schematically shown in Fig. 2 is a hollow cylinder with the ratio of length to diameter about 6:1. A carbon film is deposited onto its surface and serves both as a heater and thermometer. Specimen small mass, high thermal diffusivity and low heat capacity provide short time of temperature field equalization over the heat transfer body and low level of energy expended on the warming up. Figure 2 also illustrates the used way of confinement: the specimen is put coaxially into a thin walled tube forming an annular channel with a hot internal surface and outlets open to the fluid bath. By using tubes of different diameters it is possible to vary the degree of the coolant space restriction around the heat transfer surface. This configuration was applied earlier to study transient heat transfer into HeII under pulse heat load input^{2/}.

Loading and measurement. To meet the thermometric requirements, the dependence of the heater-thermometer resistance on the temperature is rather steep. Therefore, a

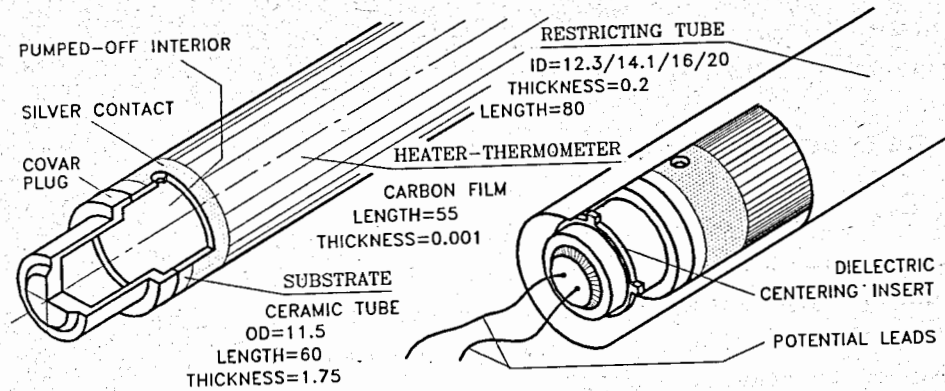


Fig.2. Test sample design (all the dimensions are in millimeters.)

special amplifier is employed to maintain the thermal power constant during the heating. The heat load duration is shorter, the stabilization is more important. The trailing edge of the power pulse initiates the sequence of probe pulses. The pulse parameters as well as a sketch of instrument set up are given in Fig. 3. The probe pulse sizes are determined with two factors crossed: the first one is the measurement convenience of the thermometer response, the second - the guarantee against the temperature disturbance.

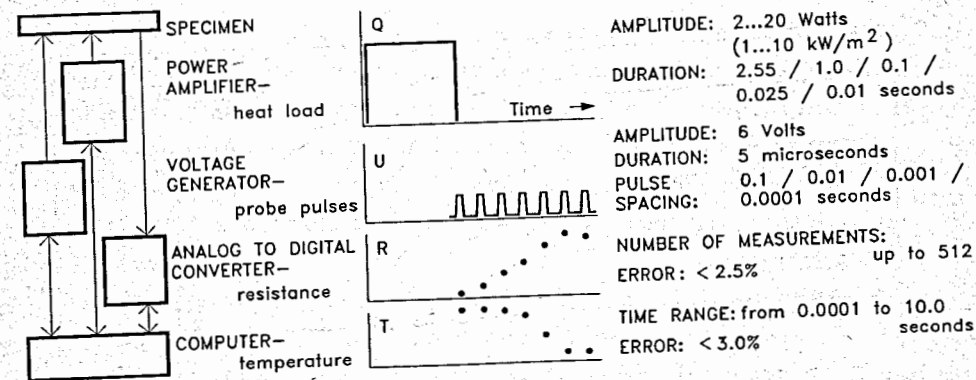


Fig.3. Sketch and parameters of the loading-measuring cluster.

This technique has been used for the preceding recovery experiment^{3/} in HeI.

RESULTS AND DISCUSSION

A package of 49 tests covers the following parameter variations: heat pulse duration - from 10 ms to 2.55 s, annular gap width - from 0.4 to 4.0 mm, bulk fluid temperature - from 1.5 to 2.2 K, specimen orientation with respect to gravity - 0/90°.

The typical results are plotted in Fig. 4 showing that the temperature of the cooled surface decreases slowly during some period of about 0.01 s and then drops to the level of HeII temperature.

To characterize quantitatively the recovery dynamics it is natural to take the moment of complete cooldown, Δt . The used method for Δt determination is illustrated in Fig. 5 and defines Δt as the intersection point between the fitting curve and the bath temperature level.

Figure 6 presents Δt as a function of the pulse power, Q , and duration, τ . It can be seen that every $\Delta t(Q; \tau)$ dependence has a bend point dividing it into two parts (e.g. for $\Delta t(Q; \tau=0.1)$ the bend point abscissa is ≈ 10 .) The left

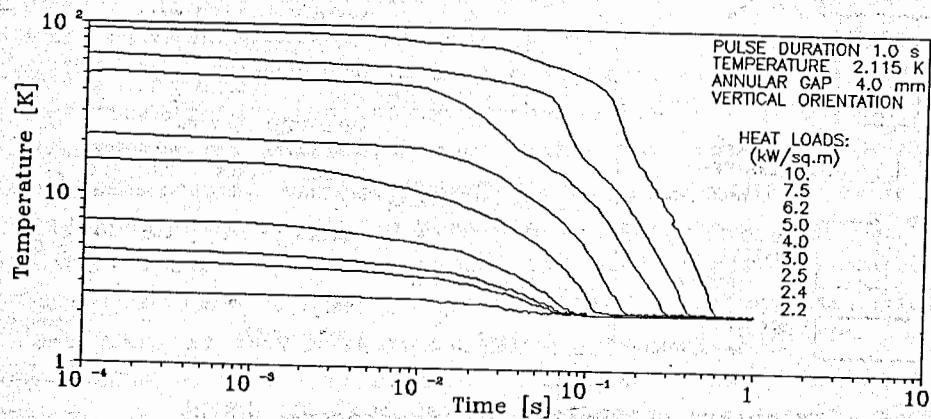


Fig.4. The decay of temperature after heat load switch-off.

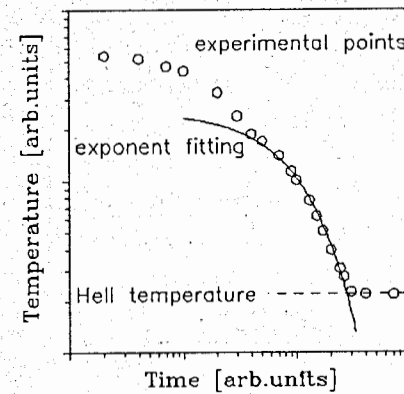


Fig.5. Determination of Δt , the complete recovery moment.

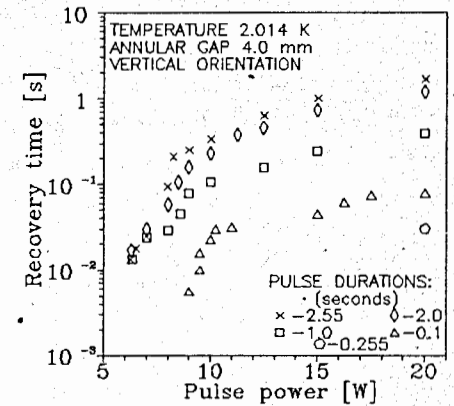


Fig.6. The dependence of Δt on heat load parameters.

part describes recovery from non-boiling heat transfer, and the right one - from the film boiling. The following empirical correlation describes the data for recovery from film boiling within 10% accuracy

$$\Delta t = \text{Const} \cdot \tau \cdot Q^2 \quad (1)$$

Figure 7 shows the Δt versus bath temperature with the unimodal shape (Δt data are normalized by the extremum ordinates.) After being averaged over all the tests the extremum abscissa equals 1.86 K and the Δt variation limit is ≈ 7 times. As Fig. 8 demonstrates, the orientation of the test sample has not a pronounced effect on the Δt while the degree of restriction is a factor causing the Δt to vary by an order.

It seems promising to consider the second dynamic characteristic - the rate of temperature decay or the relaxation constant. This quantity appears while fitting the $T(t)$ data with an exponent function $\text{Exp}[-t/D]$, see Fig. 5. The relaxation constant dependence on the heat pulse energy is shown in Fig. 9. The left and right branches of the

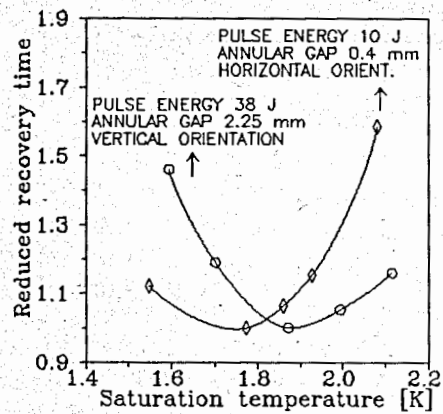


Fig. 7. The influence of bulk HeII temperature on Δt .

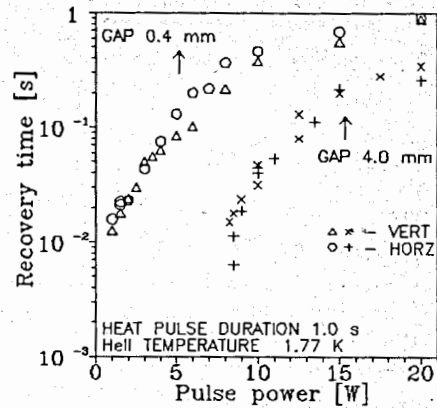


Fig. 8. The effect of restriction and specimen orientation.

$D(\tau, Q)$ curve are related to non-boiling and film boiling regimes. The negative peak corresponds to the limiting film boiling stage. This $D(\tau, Q)$ shape predicts the possibility for certain $T(t; Q)$ curves intersecting: when $Q^I < Q^J \approx Q^{EXTR}$ and $T^I \approx T^J \Rightarrow \Delta t^I > \Delta t^J$. Thus, the recovery from the non-boiling regime can proceed slower than from the limiting film boiling state if the initial temperatures are close. Such occurrences have been traced.

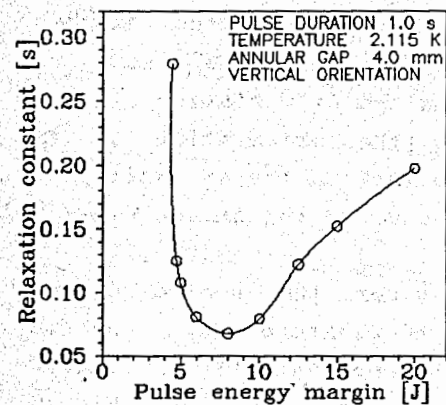


Fig. 9. Relaxation constant, D , versus applied energy.

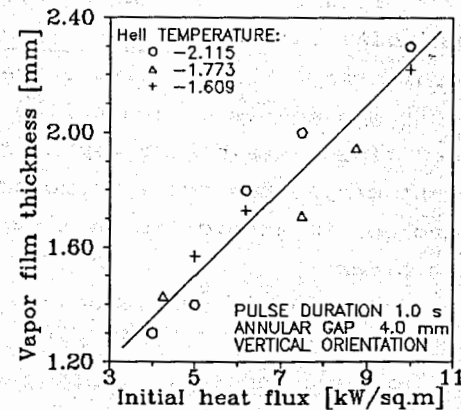


Fig. 10. Vapor film thickness, δ , versus heat load.

Besides, the vapor film thickness can be estimated. In the solid-state approximation the temperature distribution over the film can be written in the form of infinite series. This series involves the time dependent members, $\text{Exp}[-\kappa \cdot G^2 \cdot t]$, where κ is the thermal diffusivity and G - the geometric parameter. In the present case $G = \pi / (2 \cdot \delta)$, where δ is the vapor layer thickness. Comparing with the data fitting function mentioned above, one obtains

$$\delta = 2 / (\pi \cdot D \cdot \kappa^{0.5}) \quad (2)$$

where κ is averaged over the range of the fitted temperatures. Formula (2) gives a realistic magnitude of δ - of 1 mm order. The estimation results of the vapor film thickness for various heat load are given in Fig. 10. The dependence of δ on Q is approximately linear just as it was expected.

In addition, some interesting situation exists when the estimated value of vapor film thickness exceeds the width of the restricting channel. The recovery pattern under such condition is presented in Fig. 11. One can see a number of temperature irregularities and oscillations not observed

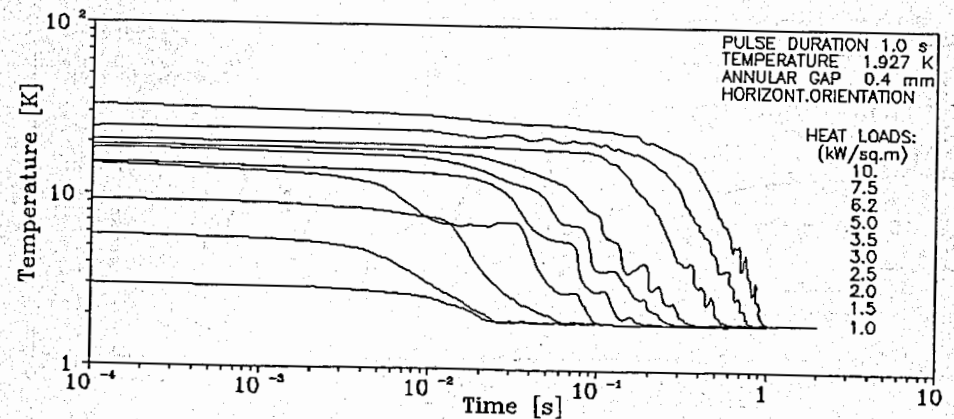


Fig. 11. The decay of temperature under confinement of high degree.

under smaller restriction degree (conf. Fig. 4). Such $T(t)$ behavior, evidently, reflects the vapor interactions with the confining channel walls and outlets.

To crown it all we should consider the heat flux variation. The $q(t)$ can be hardly measured directly. Therefore, the $q(t)$ evolution has been derived numerically from the $T(t)$ measurement results. The method is explained in the Appendix.

The typical results of $q(t)$ calculation are pictured in Fig. 12. There are four character stages of the heat flux evolution:

- the first stage is not clearly observed but can be easily imagined. To do that one can join the left upper corner of the plot with the start point of every $q(t)$ curve. This stage is a rather fast transition from the heat transfer into HeII with the generation of thermal power to the regime without heat generation;
- the second one is the region where the heat flux remains approximately stable. It means that the temperature field over the heat transfer body drifts slowly holding its own shape, i.e. the fields are self-similar. In this period the vapor film keeps overheated and stable;

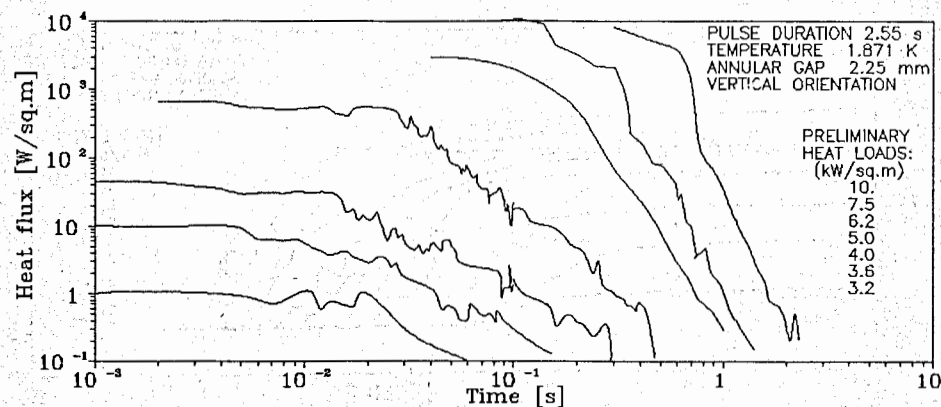


Fig.12. The evolution of heat flux into fluid helium during recovery.

- the third one covers the area on the $q-t$ chart where the heat flux decreases with time roughly according to the power law. The in-time temperature decay obeys the exponential law. Here the heat influx from the specimen to vapor becomes insufficient and the vapor film begins to cooldown;
- the fourth one corresponds to the flux falling abruptly towards zero. The simultaneous $T(t)$ function changes its shape from convex to concave and the temperature of heat transfer surface reaches the value of the bulk fluid helium temperature. During this period the vapor film collapses.

Figure 13 represents the above defined stages of recovery. It is necessary to note that the duration and, consequently, importance of any stage depends significantly on the heat transfer configuration.

Collecting all the recovery time data (Figs. 6, 7, 8 and others that have not appeared in the present paper) we have got the following partial contributions. The recovery duration is observed to be set as $\approx 70\%$ by the stage of film boiling received by the end of heat generation (i.e. by the heat pulse parameters, mainly), as $\approx 20\%$ - by the bulk HeII temperature and as $\approx 15\%$ - by the confinement degree while the heat transfer surface orientation has no pronouncing direct effect.

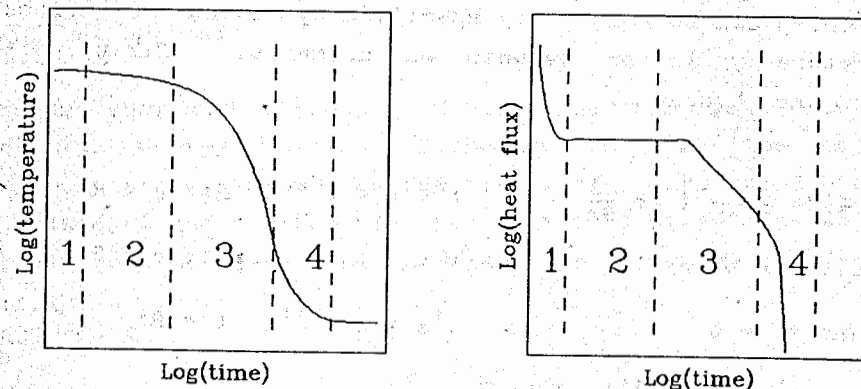


Fig.13. Stages of recovery (designations are disclosed in text).

It is impossible to derive heat flux into helium, $q(t)$, from the measurement results, $T^1(t^1) \dots T^K(t^K), T^{K+1}(t^{K+1}) \dots$, immediately. Preliminary, one should calculate instantaneous temperature field over a heat transfer solid, $Z(r, x, \varphi, t)$. The problem is formulated and solved below.

Specimen design, Fig. 2, allows the following ad hoc assumptions:

- thermometer enthalpy is negligible due to its extremely small thickness \Rightarrow heat is emitted into helium from the substrate only;
- the interior is pumped-off \Rightarrow the heat flux vanishes on the inner substrate surface;
- thermal resistance of the substrate-thermometer interface is low due to intimacy of contact (deposition) and similarity of matter structures (both amorphous) \Rightarrow the temperature of substrate outer surface coincides with the measured one;
- thermometer readouts represent the volume integral, therefore the measured temperature is the mean value over the substrate surface \Rightarrow the angular coordinate, φ , has to be discarded;
- longitudinal heat flow is small (as estimated, does not exceed 5%) \Rightarrow axial coordinate, x , may be ignored.

The problem can be completely specified by giving the surface temperature variation between measurements. Taking it linear, one obtains

$$\left\{ \begin{array}{l} \rho c \frac{\partial Z}{\partial t} = \frac{1}{r} \frac{\partial}{\partial r} \left(\lambda r \frac{\partial Z}{\partial r} \right) ; \quad t^K < t < t^{K+1}, \quad R_i < r < R_o \\ Z(r, t^K) = W^K(r) ; \quad t^K = t, \quad R_i \leq r \leq R_o \\ \frac{\partial Z}{\partial r}(R_i, t) = 0 ; \quad t^K \leq t \leq t^{K+1}, \quad r = R_i \\ Z(R_o, t) = T^K + \frac{(T^{K+1} - T^K) *}{(t - t^K) / (t^{K+1} - t^K)} ; \quad t^K \leq t \leq t^{K+1}, \quad r = R_o. \end{array} \right. \quad (A.1)$$

where R_i and R_o are the inside radius and the outside one, respectively. The thermophysical properties ρ , c , λ are considered to be constant within the current time interval $[t; t^{K+1}]$ though recalculated at some average temperature, θ , for every other interval $[t^{K+1}; t^{K+2}]$. The value of θ is defined as $(W^{K+1}(R_i) + T^{K+2}(t^{K+2}))/2$.

This problem is analogous to that one being under consideration in the book⁴ for a flat case. Set (A.1) integrates to the following expression

$$Z(r, t) = T^K + (t - t^K) \frac{T^{K+1} - T^K}{t^{K+1} - t^K} + \sum_{j=1}^{\infty} A_j B_j(r) C_j(t) + \sum_{i=1}^{\infty} A_i^* B_i(r) C_i^*(t)$$

where the space dependent members $B(r)$ represent a linear combination of Bessel functions, the time dependent members $C(t)$ involve exponents, and the coefficients A include integrals $\int B(r) W(r) r dr$ taken from R_i to R_o as well as normalizing factors.

As soon as $Z(r, t^K) = W^{K+1}(r)$, the temperature field for any instant can be found with the *step by step* procedure assuming the zero-point-field to be uniform, $Z(r, t^0) = W^1(r) = T^1$. Consequently, the heat flux $q(t^K)$ can be calculated for every experimental point $T(t^K)$.

ACKNOWLEDGEMENTS

We are very much obliged to E. Suslov and M. Priyma (Institute of High Energy Physics, Serpukhov SU) for the pressure stabilization system. We are also grateful to our colleagues V. Miklayev and V. Minashkin for their contribution to the equipment adjustment and experiment performance.

REFERENCES

1. S. W. Van Sciver, Correlation of time dependent recovery from film boiling heat transfer in HeII, Cryogenics

21:529 (1980).

2. Yu. P. Filippov, V. M. Miklayev, and I. A. Sergeev, Transient heat transfer into superfluid helium under confined conditions, in: " Proc. Twelfth Int. Cryo. Engr. Conf.," Butterworth, Guildford UK (1988), p. 290.
3. Yu. P. Filippov and I. A. Sergeev, Transient thermal recovery of preheated solid in a liquid helium bath - 1st report, in: "Proc. Low Temperature Engineering and Cryogenics Conf.," Institute of Cryogenics, Southampton UK (1990), p. 11.3.
4. H. S. Carslaw and J. C. Jaeger, " Conduction of Heat in Solids," Oxford University Press, Oxford UK (1950).

Received by Publishing Department
on August 2, 1991.

Филиппов Ю.П., Сергеев И.А.

E8-91-369

Динамика возврата из режима пленочного кипения HeII в стесненных условиях

Приведены результаты экспериментального исследования динамики остывания твердого тела в объеме насыщенного сверхтекучего гелия после выключения тепловой нагрузки. Особенность изучавшейся конфигурации теплопередачи состоит в ограничении пространства у охлаждаемой поверхности. Найдено, что длительность релаксации определяется \approx \approx на 70% развитостью стадии пленочного кипения, достигнутой к окончанию нагрева, \approx на 20% величиной температуры объема гелия, \approx на 15% степенью стеснения. Ориентация образца не имеет непосредственного влияния на время релаксации.

Работа выполнена в Лаборатории сверхвысоких энергий ОИЯИ.

Препринт Объединенного института ядерных исследований. Дубна 1991

Filippov Yu.P., Sergeev I.A.

E8-91-369

Time-Dependent Recovery from Hell Film Boiling: Confined Geometry Case

Experiment results for transient cooldown of a solid in saturated superfluid helium after heat load switch-off are reported. The fluid space restriction in the vicinity of a heater is a specific feature of the tested heat transfer configuration. In this case the recovery duration is found to be set as \approx 70% by the stage of film boiling received by the end of heat generation, as \approx 20% - by the value of bulk fluid temperature, as \approx 15% - by the confinement degree. The sample orientation does not affect the recovery time directly.

The investigation has been performed at the Particle Physics Laboratory, JINR.

Preprint of the Joint Institute for Nuclear Research. Dubna 1991